Wnt/β-Catenin coordinates muscle spindle development by regulating capsule differentiation, intrafusal fiber nuclei aggregation and proprioceptive nerve endings

Qingyuan Guo[1], Ava Gatterer[1], Avital Rosner[1], Sharon Krief[1], Ron Rotkopf[2], Fabian S. Passini[1], Noa Wigoda[2], Bavat Bornstein[1] Elazar Zelzer[1]

[1]Weizmann Institute of Science, Department of Molecular Genetics, Rehovot 76100, Israel
[2]Bioinformatics Unit, Department of Life Sciences Core Facilities, Weizmann Institute of Science, Rehovot, 76100, Israel

Corresponding Authors: Eli.Zelzer@weizmann.ac.il

Abstract

Proprioception is essential for regulating posture, coordinating movements, and maintaining musculoskeletal integrity. The muscle spindle, a mechanosensory organ composed of several types of tissues, detects stretch, forming proprioceptive awareness. Despite its significance, the molecular mechanisms underlying the coordinated development of the different tissues composing the spindle remain unclear.

Here we show that Wnt ligands and their Fzd receptors are expressed in the developing spindle. Similarly, β-catenin is active in both the spindle capsule and intrafusal fibers throughout their development. Embryonic deletion of β-catenin from these tissues impaired capsule cell differentiation, intrafusal fiber nuclei organization, and proprioceptive nerve ending morphology. Postnatal deletion of β-catenin solely in intrafusal fibers results in abnormal proprioceptive nerve endings, suggesting both cell-autonomous and cell-non-autonomous roles of β-catenin in muscle spindle development. Our subsequent RNA transcriptome analysis of the β-catenin mutant spindle not only provides a molecular mechanism underlying the role of β-catenin in spindle development, but also expands the repertoire of molecules involved in spindle biology. By exposing a vast repertoire of new molecules involving all spindle tissues, our transcriptome could serve as a resource and benchmark for future discoveries in spindle biology.

Collectively, our findings position the Wnt/β-catenin pathway as a central regulator with cell-autonomous and cell-non-autonomous roles, coordinating the diverse tissues of the spindle into a functional organ. Our transcriptome data further provide insight into spindle biology through a set of newly discovered molecules.

Introduction

The proprioceptive system reports on the relative position and movement of body parts and is therefore essential for control and coordination of movement and posture[1]. In humans, loss of proprioception leads to compromised sensory and motor control resulting in ataxia, abnormal gait, and difficulties in identifying the position of body parts[2]. Furthermore, in recent years, studies in mice show that proprioceptive dysfunction contributes to various musculoskeletal pathologies, including scoliosis, hip dysplasia, and joint contractures[3-6].

A central component of the mammalian proprioceptive system is the muscle spindle, a small mechanosensory organ that is sparsely embedded within skeletal muscles. The spindle detects changes in muscle length and transmits this information to the central nervous system to establish proprioceptive awareness[7-8]. A muscle spindle is a complex organ composed of specialized muscle fibers, termed intrafusal fibers, which are innervated by proprioceptive sensory neurons at their central region and by γ-motor neurons at their polar ends. Intrafusal fibers are classified by their nuclear organization and function into three types: bag1, bag2, and chain fibers. The spindle is partially isolated from its surroundings by a capsule rich in extracellular matrix (ECM) that is secreted by capsule cells[7-8].

Muscle spindle development begins around embryonic day 14 (E14), when slow myofibers first contact proprioceptive axons and differentiate into intrafusal fibers in a sequential process[8]. First, nuclear bag fibers are formed, followed by the formation of nuclear chain fibers[9]. In coordination with fiber differentiation, proprioceptive neurons undergo maturation. This morphogenetic process transforms a web-like network into a complex structure termed the annulospiral ending, where neurons wrap around the center of each intrafusal fiber[10]. Capsule development also involves progressive waves of cell differentiation, moving from the center of the spindle to its sides[11]. We know little about spindle development at the molecular level. Neuregulin 1 (NRG1), expressed by sensory neurons, activates ErbB2 signaling in myofibers to induce the intrafusal genetic program. In return, neurotrophin-3 expressed by intrafusal fibers activates the tropomyosin receptor kinase C (TrkC) receptor on proprioceptive sensory neurons, which is necessary for their survival[12-16]. Recent work has shown that LRP4 expression in intrafusal fibers is necessary to maintain the sensory synapses of annulospiral endings and thereby proprioceptive function[17]. Nevertheless,

molecular mechanisms underlying the coordinated development of the different tissues forming the spindle are unknown.

Wnt/β-catenin signaling is a central pathway that regulates a variety of cellular processes during development, including cell fate determination, migration, and polarity, as well as tissue homeostasis, regeneration, and pathology. The pathway is activated when Wnt ligands bind to their membrane receptors Frizzled and LRP5/6. This interaction results in the translocation of β-catenin to the nucleus, where it activates transcription of target genes by interacting with TCF/LEF transcription factors[18-19]. Interestingly, Wnt7A expression is detected in γ-motor neurons of the muscle spindle, whereas Frizzled 5 is expressed in the capsule[20]. These observations suggest that Wnt/β-catenin signaling may be involved in spindle development.

In this study, we find both Wnt ligands and Fzd receptors to be expressed in different spindle tissues. Moreover, we find persistent activation of Wnt/β-catenin in capsule and Bag2 intrafusal fibers throughout spindle development. Embryonic deletion of β-catenin from both capsule and intrafusal fibers reduces differentiation of capsule cells, disrupts intrafusal fiber nuclear organization, and causes disorganization of proprioceptive nerve endings. The latter also occurs upon postnatal deletion from muscle fibers alone, indicating both cell autonomous and non-autonomous regulation of β-catenin during spindle development. Our RNA-seq analysis identifies molecular mechanisms for Wnt/β-catenin regulation of spindle development and reveals novel muscle spindle genes. Collectively, our findings identify a new function of β-catenin in the regulation of spindle development and implicate numerous previously unknown genes in spindle biology.

Results

The Wnt/ β-catenin pathway is active in muscle spindles throughout development

To identify potential molecular pathways that regulate spindle development, we applied Ingenuity Pathway Analysis (IPA)[21] on RNA-seq data we recently obtained from spindles[11]. We identified numerous upstream regulators of genes enriched in spindles, including the top candidates *Pou4f1, Dnmt3b,* and *Ctnnb1* (Table S1). *Ctnnb1*'s protein product β-catenin is a central intracellular signal transducer in the Wnt signaling pathway[18-19]. Indeed, IPA reveals enrichment of multiple components of the Wnt/β-catenin pathway (Figure 1A), including Wnt ligands, Frizzled receptors, and TCF/LEF transcription factors (Figure 1B). These results suggest an important role for Wnt/β-catenin signaling in spindle development.

Our transcriptomic analysis reveals upregulated expression of several Wnt ligands (*Wnt1, Wnt2b, Wnt3, Wnt6, Wnt7b and Wnt10a, Wnt10b, Wnt16)* and Frizzled receptors (*Fzd1, Fzd2, Fzd3, Fzd5, Fzd9* and *Fzd10)* in muscle spindles (Table S2). To validate these results and to determine the spatial distribution of some of these molecules, we applied HCR to frozen sections from deep masseter muscles and whole-mount extensor digitorium longus (EDL) muscles. To outline the various spindle tissues, we used *Gli1-CreER^{T2};TdTomato* to mark capsule cells[11] (Figure 1C-H) and *Calb1-Cre;TdTomato* to mark intrafusal fibers[22] (Figure S1). *Wnt2b*, *Wnt6,* and *Fzd2* are expressed by capsule cells (Figure 1C-E), whereas *Wnt7b* and *Fzd10* are expressed by intrafusal fiber cells (Figure 1F-G, Figure S1A, C). *Wnt10a* is expressed in both capsule cells and intrafusal fibers (Figure 1H, Figure S1B).

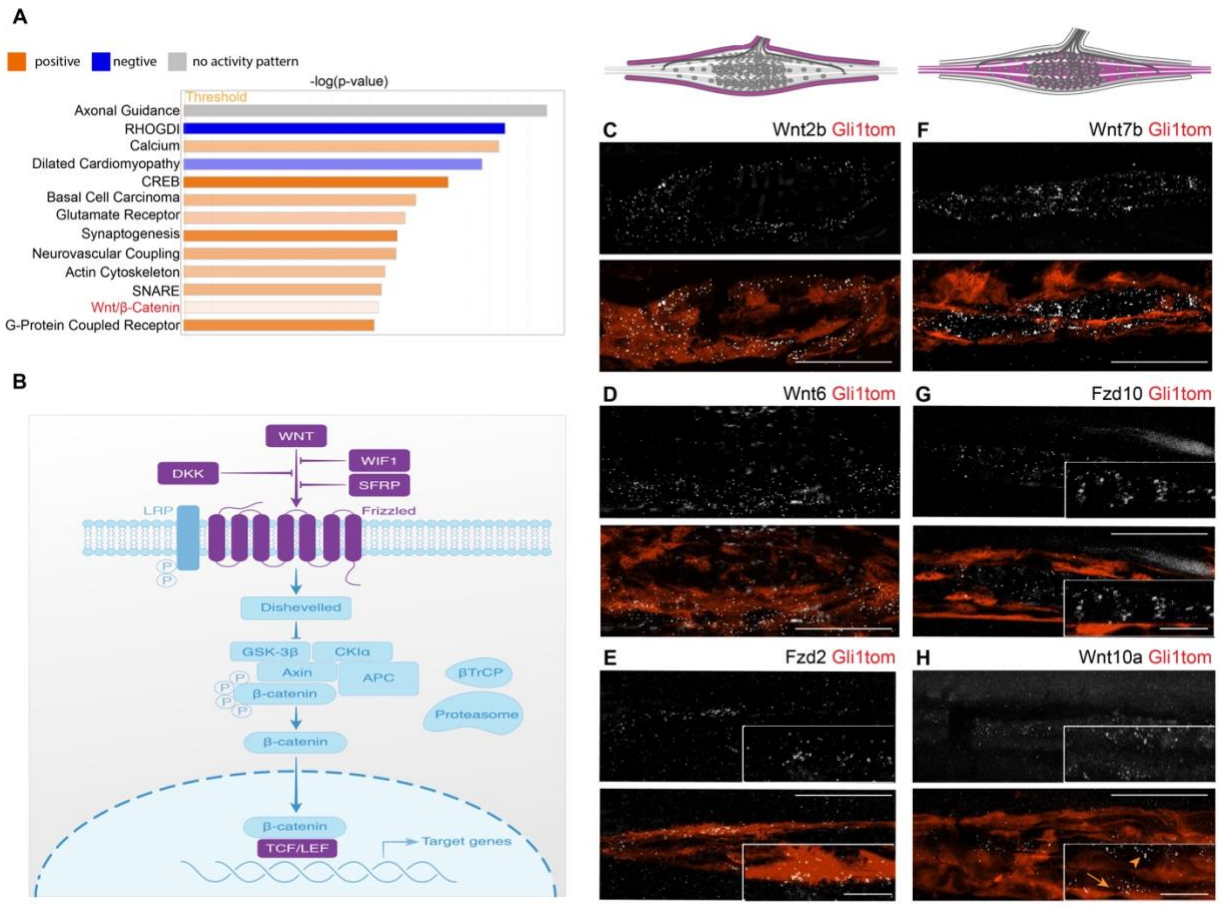

Figure 1. Transcriptomic and expression analysis reveals expression of Wnt/β-catenin pathway components in muscle spindles. (A) Ingenuity Pathway Analysis of differentially expressed genes (DEG) between muscle spindle and muscle samples. (B) Schematic representation of Wnt/β-catenin pathway. Purple blocks represent genes upregulated in spindles compared to muscles. (C-H) Confocal images of longitudinal sections of deep masseter muscles (C-D, F, H) and whole-mount of EDL muscles (E, G) from P33 *Gli1-CreER^{T2},Rosa26-tdTomato* mice. Expression of the indicated Wnt/β-catenin pathway genes was detected by HCR probes following tamoxifen administration at P26. *Wnt2b*, *Wnt6* and *Fzd2* are expressed in capsule cells (C-E) with enlarged image for *Fzd2* (E), *Wnt7b* and *Fzd10* are expressed in intrafusal fibers (F,G) with enlarged image for *Fzd10* (G), and *Wnt10a* is expressed in both (H) with enlarged image. Arrow points at capsule expression and arrowhead points at intrafusal expression. Top: schematic representation of muscle spindles show in purple the tissue in which the indicated genes were expressed. Scale bars: 100 μm for enlarged images, and 50 μm for the rest.

To directly study Wnt/β-catenin pathway activity in the developing spindle, we used *Axin2*-membrane GFP (mGFP) reporter mice. *Axin2* is a direct target of Wnt/β-catenin, and *Axin2-mGFP*

mice report pathway activity faithfully[23]. As seen in Figure 2A, we detect GFP signal in both extrafusal fibers and muscle spindles at postnatal day 0 (P0) and P5. At P25 and P40, the GFP signal is lost in extrafusal fibers but maintained in muscle spindles. To determine the spindle cell types in which Wnt signaling is active, we stained EDL muscles from *Axin2-mGFP* mice using antibodies against MyHC7B and Glut1, markers for bag2 fiber and capsule cells, respectively[11, 24]. As shown in Figure 2B-C and Figure S2, at all stages of development, Wnt/ β-catenin activity is specific to bag2 fibers and capsule cells. Overall, these results show that Wnt signaling is active and ongoing in developing spindles.

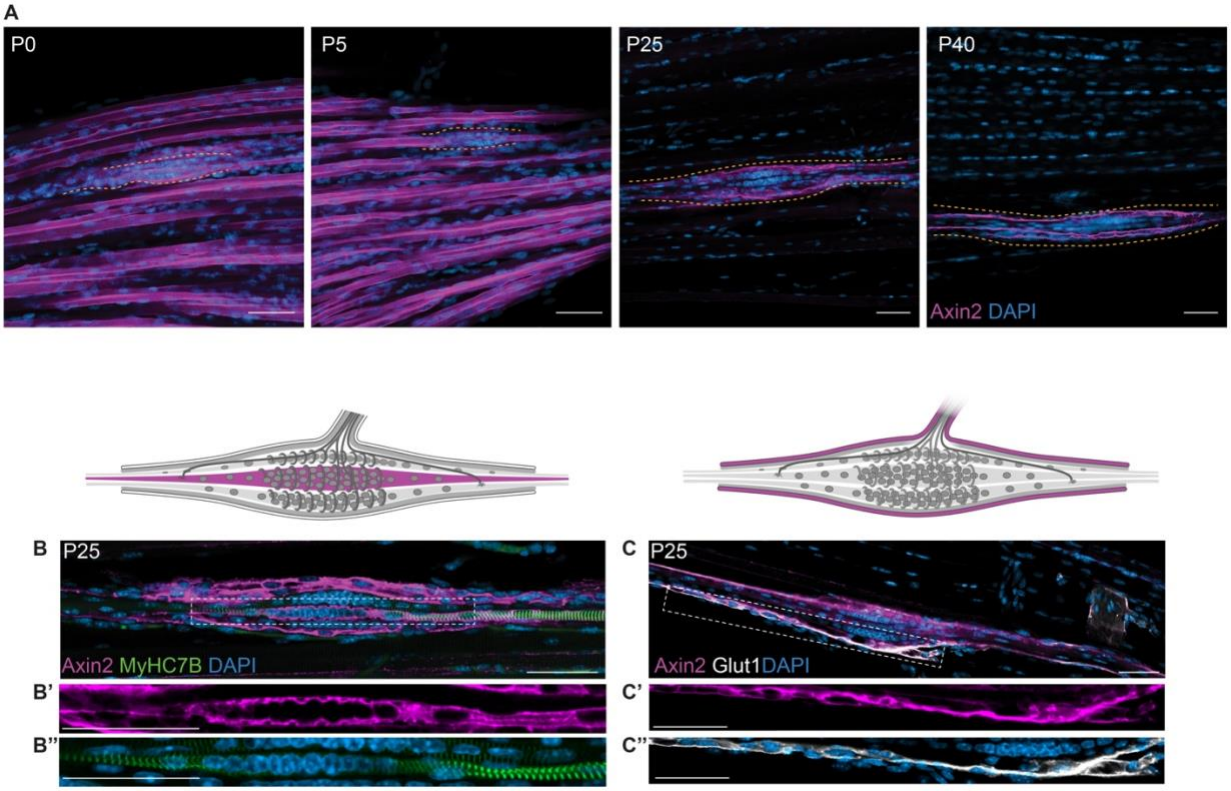

Figure 2. β-catenin activity is detected in muscle spindles throughout development. (A) Confocal images of whole-mount EDL muscles from P0, P5, P25 and P40 *Axin2-mGFP* mice stained with antibodies against GFP (magenta) and DAPI (blue). Dotted lines demarcate equatorial region of spindles. Scale bars: 50 μm. (B-C'') Confocal images of whole-mount EDL muscles from P25 *Axin2-mGFP* mice stained with antibodies against GFP, DAPI and MyHC7B (green, B-B'') or Glut1 (white, C-C''). Above are schematic representations of muscle spindles with the tissue analyzed in purple. Scale bars: 50 μm.

151 **Embryonic β -catenin is necessary for muscle spindle development**

152

153 To directly test the hypothesis that Wnt/β-catenin pathway regulates muscle spindle development,
154 we deleted β-catenin from both intrafusal fibers and capsule cells using *Egr3*^{Cre} mice, in which Cre
155 recombination is induced in these cells[25]. *Egr3*^{Cre}, β-*catenin*$^{loxP/+}$ mice were crossed with β-
156 *catenin*$^{loxP/loxP}$ mice[26]. β-catenin mutants were born at the expected ratio; however, during postnatal
157 growth, mutants appeared smaller, lacked fur and died by P30.

158

159 Given that muscle spindles largely acquire adult morphology by P25[8,11], we studied the effect of
160 β-catenin loss in P25 mice. First, we examined capsule development by analyzing the expression
161 of GLUT1 and VCAN, markers for early and advanced capsule differentiation, respectively[11]. As
162 shown in Figures 3A and 3E, we detect GLUT1 expression in control spindles throughout the
163 muscle spindle, whereas in mutant spindles its expression is restricted to the equatorial region.
164 Moreover, unlike in controls, VCAN expression is almost absent in mutant spindles (Figure 3B),
165 suggesting that capsule cells failed to differentiate. Finally, the distance between GLUT1+ layers
166 is smaller, indicating a thinner muscle spindle in mutants (Figure 3E')

167

168 Next, we examined intrafusal fiber development, by analyzing the typical morphological feature
169 of nuclear organization at the equatorial regions of bag fibers[7-8]. We find that nuclear organization
170 in mutant bag2 fibers is clearly abnormal, marked by abnormal aggregation in the equatorial region.
171 By contrast, nuclear aggregation in mutant bag1 fibers is comparable to wild type (Figure 3C, C',
172 F). Collectively and in agreement with the observed activation patterns of β-catenin, these results
173 suggest that β-catenin is necessary for bag2 fiber development.

174

175 Finally, we studied the development of the annulospiral endings of type Ia proprioceptive neurons,
176 which innervate intrafusal fibers, using an antibody against ATP1a3[11]. As seen in Figure 3D-D',
177 while proprioceptive neurons of control mice exhibit stereotypical annulospiral loops, β-catenin
178 mutant spindles show abnormal morphology (Figure 3G-G'). Quantification reveals loops with
179 similar width, but with reduced number of loops and increased distance between loops in both
180 bag1 and bag2 fibers (Figure 3G-G''). Interestingly, these morphological alterations are more
181 severe in annulospiral endings innervating bag2 fibers than in those innervating bag1 fibers.

182 Overall, our findings indicate that Wnt/ β-catenin activity is necessary for the development of all
183 spindle tissues, including the capsule, intrafusal fibers, and proprioceptive neuron, suggesting both
184 cell-autonomous and cell-non autonomous roles of β-catenin.

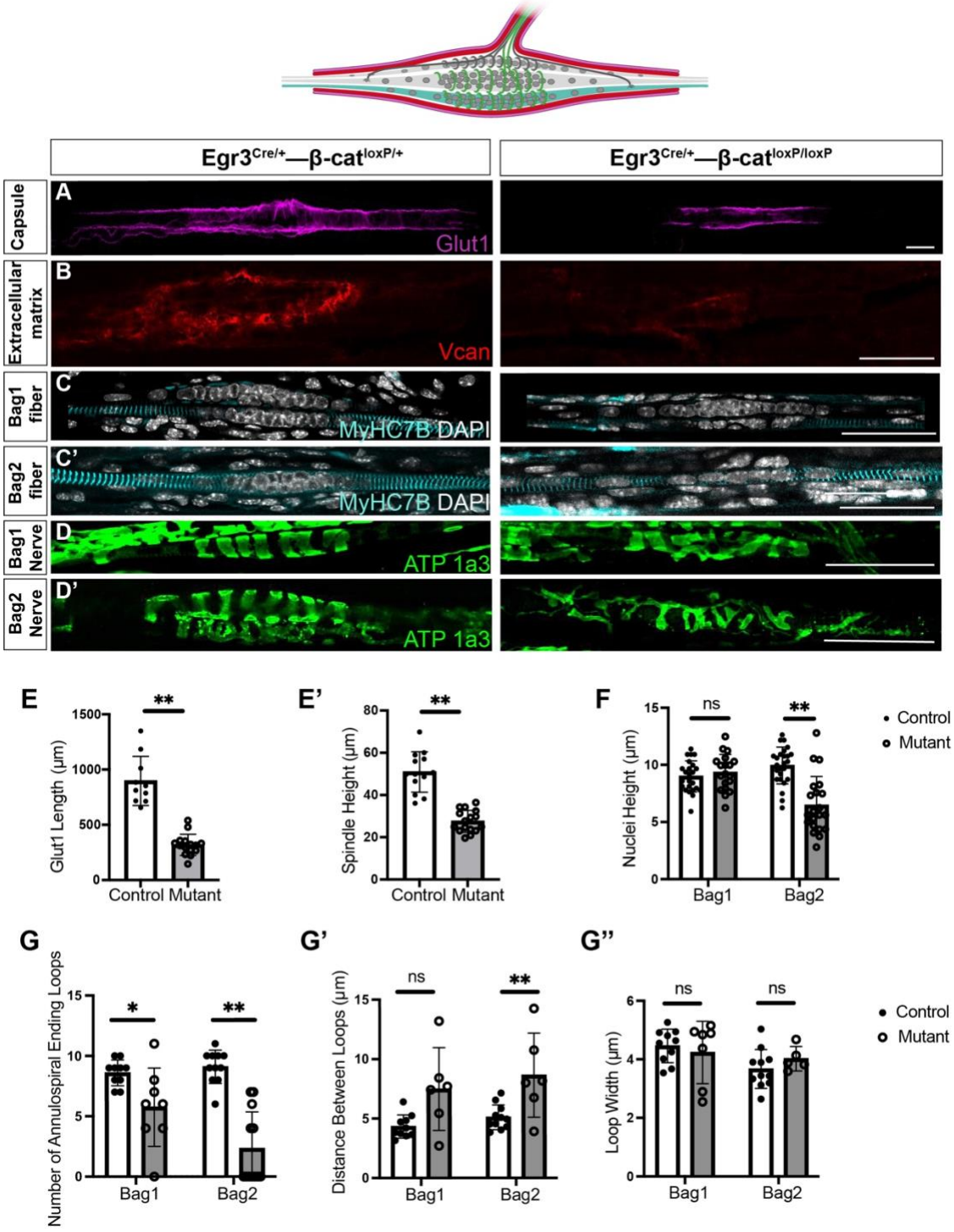

185

186 **Figure 3. Deletion of β-catenin from capsule and intrafusal fibers results in morphological**
187 **abnormalities in three spindle tissues.** (A-D') Confocal images of P25 muscle spindles from
188 mice of the indicated genotypes. Capsules were stained with anti-GLUT1 antibodies in whole-
189 mount gluteus muscles, ECM was stained with anti-VCAN antibodies in longitudinal sections
190 from deep masseter muscles, bag2 intrafusal fibers were stained with anti-MyHC7B antibodies
191 in whole-mount EDL muscles, and proprioceptive neurons were stained with anti-ATP 1a3
192 antibodies in whole-mount gluteus muscles. Scale bars: 50 μm. (E) GLUT1 expression was
193 restricted to the equatorial regions in mutants (**P<0.01, n=3). Gluteus muscles were used for
194 quantification. (E') Decreased distance between GLUT1^{+} capsule layers indicates a shorter
195 spindle height in mutants (**P<0.01, n=3). Gluteus muscles were used for quantification. (F)
196 Abnormal nuclear aggregation and shorter nucleus height in the equatorial regions of mutant
197 intrafusal fibers (**P<0.01, n=3). EDL muscles were used for quantification. (G-G'') Although
198 the width of annulospiral endings was not affected, the distance between loops and the number of
199 loops per spindle was decreased in mutants (**P<0.01, *P<0.05, n=3). EDL muscles were used
200 for the quantification.
201

202 **Postnatal deletion of β-catenin in intrafusal fibers leads to abnormal annulospiral endings**
203
204 Persistent β-catenin activity throughout spindle development strongly suggests its necessity past
205 the embryonic stage. To test this possibility directly and to uncover the possible regulatory role of
206 β-catenin in the postnatal spindle, we used the *HSA*^{CreER} line[27], which allows temporal targeting of
207 extrafusal and intrafusal fibers. Previous postnatal studies using this line to delete β-catenin have
208 not identified a major phenotype in the extrafusal fibers[28]. We therefore expected that any spindle
209 phenotype will represent a postnatal, direct role of β-catenin in intrafusal fibers.
210
211 We crossed *HSA*$^{CreER/+}$, *β-catenin*$^{loxP/+}$ mice with *β-catenin*$^{loxP/loxP}$ mice, then administered
212 tamoxifen at P5 before collecting spindles at P25. As shown in Figure 4A-B, the pattern and level
213 of both capsule markers, GLUT1 and VCAN, is unaffected in *β*-catenin mutant mice. Similarly,
214 the distance between GLUT1+ layers is normal, indicating that the capsule of *HSA*^{CreER}*-β-catenin*
215 mutant spindles develops normally (Fig. 4E-E'). We compared intrafusal fibers between control
216 and mutant spindles and find no difference in nuclear aggregation (Fig. 4C,C', F). Interestingly,
217 however, mutant annulospiral endings innervating bag2 fibers are abnormal, with fewer and more
218 spaced loops, while annulospiral endings of bag1 fibers are intact (Fig. 4D,D', G-G''). These

219 results suggest that β-catenin activity in intrafusal fibers is necessary for the postnatal integrity of
220 the proprioceptive neuron annulospiral endings.

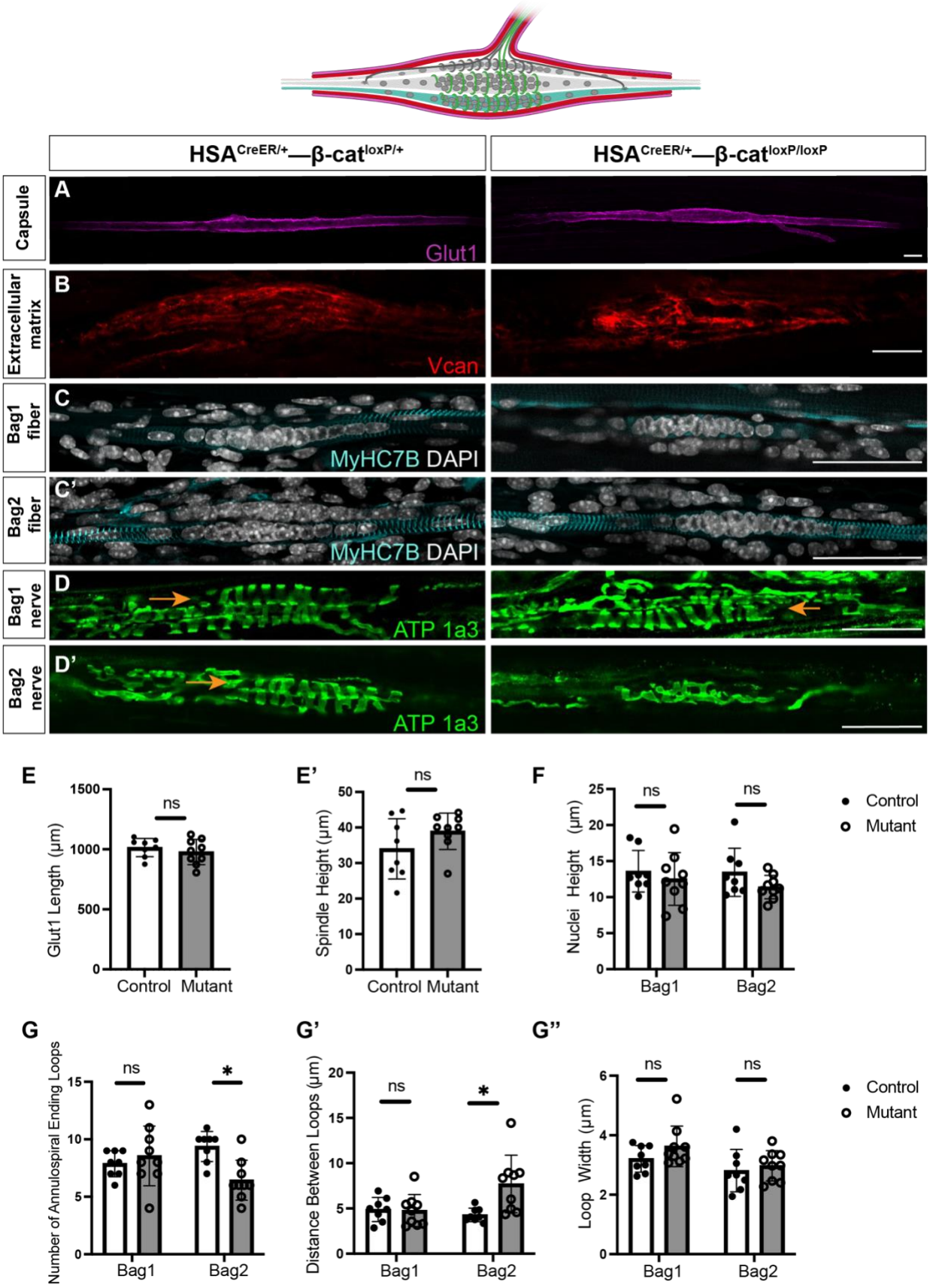
HSA CreER/+—β-cat loxP/+
HSA CreER/+—β-cat loxP/loxP
Capsule
Extracellular matrix
Bag1 fiber
Bag2 fiber
Bag1 nerve
Bag2 nerve
A
Glut1
B
Vcan
C
MyHC7B DAPI
C'
MyHC7B DAPI
D
ATP 1a3
D'
ATP 1a3
E
Glut1 Length (µm)
ns
Control
Mutant
E'
Spindle Height (µm)
ns
Control
Mutant
F
Nuclei Height (µm)
ns
ns
Bag1
Bag2
Control
Mutant
G
Number of Annulospiral Ending Loops
ns
*
Bag1
Bag2
G'
Distance Between Loops (µm)
ns
*
Bag1
Bag2
G''
Loop Width (µm)
ns
ns
Bag1
Bag2
Control
Mutant

221

222 **Figure 4. Postnatal deletion of β-catenin from intrafusal fibers results in disorganized**
223 **annulospiral endings.** (A-D') Confocal images of muscle spindles from whole-mount EDL
224 muscles of mice with indicated genotypes unless specified. Capsules were stained with anti-
225 GLUT1 antibodies, ECM was stained with anti-VCAN antibodies in longitudinal sections from
226 deep masseter muscles, bag2 intrafusal fibers were stained with anti-MyHC7B antibodies, and
227 proprioceptive neurons were stained with ATP 1a3 antibodies. Arrows point at bag1 fiber in (D)
228 and bag2 fiber in (D'). Scale bars: 50 μm. (E-F) Expression of GLUT1, spindle height as
229 measured by the distance between $GLUT1^+$ capsule layers, and nuclear aggregation in intrafusal
230 fibers were not significantly different between controls and mutants (n=3). (G-G'') Although the
231 width of annulospiral endings was similar, the distance between loops and the number of loops
232 per spindle was decreased in mutants (*P<0.05, n=3).
233
234
235 **Loss of β-catenin in the spindle results in extensive transcriptional changes across various**
236 **spindle tissues**
237
238 To provide a molecular understanding for the abnormal development of β-catenin mutant spindles,
239 we compared the transcriptomes of *Egr3-β-catenin* mutant and control spindles. The extensive
240 impact of losing β-catenin expression on spindle development suggests that deletion affects
241 expression of a broad range of genes. Moreover, since most of the molecular components of the
242 spindle remain poorly understood, identifying these genes will not only enhance our understanding
243 of β-catenin's function but also provide a list of numerous previously unknown genes essential for
244 spindle biology. Given that $Egr3^{Cre}$ also targets β-catenin in other tissues, including the interstitial
245 cells surrounding extrafusal fibers (Figure S3), we compared samples of extrafusal fibers from
246 both lines to filter out differentially expressed genes (DEG) that are not spindle-specific.
247
248 Using principal components analysis (PCA), we find different transcriptional states in control and
249 β-catenin mutant spindles (Figure S4A). In addition, we observe separation between control and
250 mutant muscle samples. Differential expression analysis revealed 747 differentially downregulated
251 and 297 upregulated genes in mutant spindles, as compared to the control (Figure S4B), indicating
252 differential molecular signatures between control and β-catenin mutant spindles.
253
254 Next, to identify spindle-specific transcriptional changes, we performed K-means clustering of all
255 DEGs in spindles and muscle samples using Partek[29]. As seen in Figure 5A, cluster 1 includes 418

256 spindle-specific downregulated genes, whereas cluster 7 includes 65 upregulated genes (Table S3).
257 In other five resulting clusters, similar gene expression changes between control and mutant
258 samples of spindles and extrafusal muscle tissues. This similarity suggests a global effects of β-
259 catenin deletion in other non-spindle tissues, for example the interstitial cells surrounding the
260 extrafusal fibers, as a result of *Egr3* expression in these cells.
261
262 To associate the observed transcriptional changes with the various spindle tissue types, we next
263 crossed-referenced the list of downregulated spindle-specific genes in cluster 1 with published
264 tissue type-specific transcriptomic data[11]. We identified 64 extracellular genes, 46 proprioceptive
265 neuron genes, and 10 intrafusal genes (Figure 5B and Table S4). GO terms and enriched pathway
266 analysis of these genes reveals terms like "extracellular matrix" and "collagen trimer" for
267 extracellular space genes, "neuron projection morphogenesis" and "positive regulation of synaptic
268 transmission" for proprioceptive neuron genes, and "neuron projection morphogenesis" and
269 "transporter complex" for intrafusal genes. Reduced expression of genes and associated GO terms
270 from all spindle tissue types is consistent with our finding that Wnt/*β*-catenin activity is necessary
271 for the development of all these tissues (Figure 3).
272
273 To validate the results and to obtain spatial information, we performed HCR on tissue-specific
274 candidate genes identified by the transcriptomic analysis. Starting with capsule genes, we verified
275 the expression of two novel spindle genes: *Gjb2,* a membrane protein that facilitates cell-to-cell
276 communication and mediates glucose transport[30]; and the retinol transporter STRA6, which binds
277 retinol-binding proteins[31]. As indicated by our bioinformatic analysis, expression of these top
278 DEGs in the β-catenin mutant spindle is reduced (Figure 5C and Figure S4C). Another novel
279 spindle gene, nerve growth factor receptor (NFGR), known to be important for axon guidance, was
280 indicated by our analysis to be expressed by the intrafusal fibers and proprioceptive neurons
281 (Figure 5C and Figure S4C). Interestingly, our transcriptomic data also identify genes encoding
282 Ngfr ligands, such as *Ngf, Bdnf, Ntf3,* and *Ntf5*[32], to be expressed in spindles, supporting a role for
283 this receptor in proprioceptive neuron development. We validated expression of *Ngfr* in the
284 equatorial region of muscle spindles, and identified reduced *Ngfr* expression in β-catenin mutant
285 spindles (Figure 5C'). Another new gene we predicted to be expressed in the intrafusal fibers is
286 *Klhl6* that is known to be important for B-cell survival and maturation[33]. As can be observed in

Fig. 5C'', we confirm both the expression of *Klhl6* in the equatorial region and its reduction in the β-catenin mutant spindle.

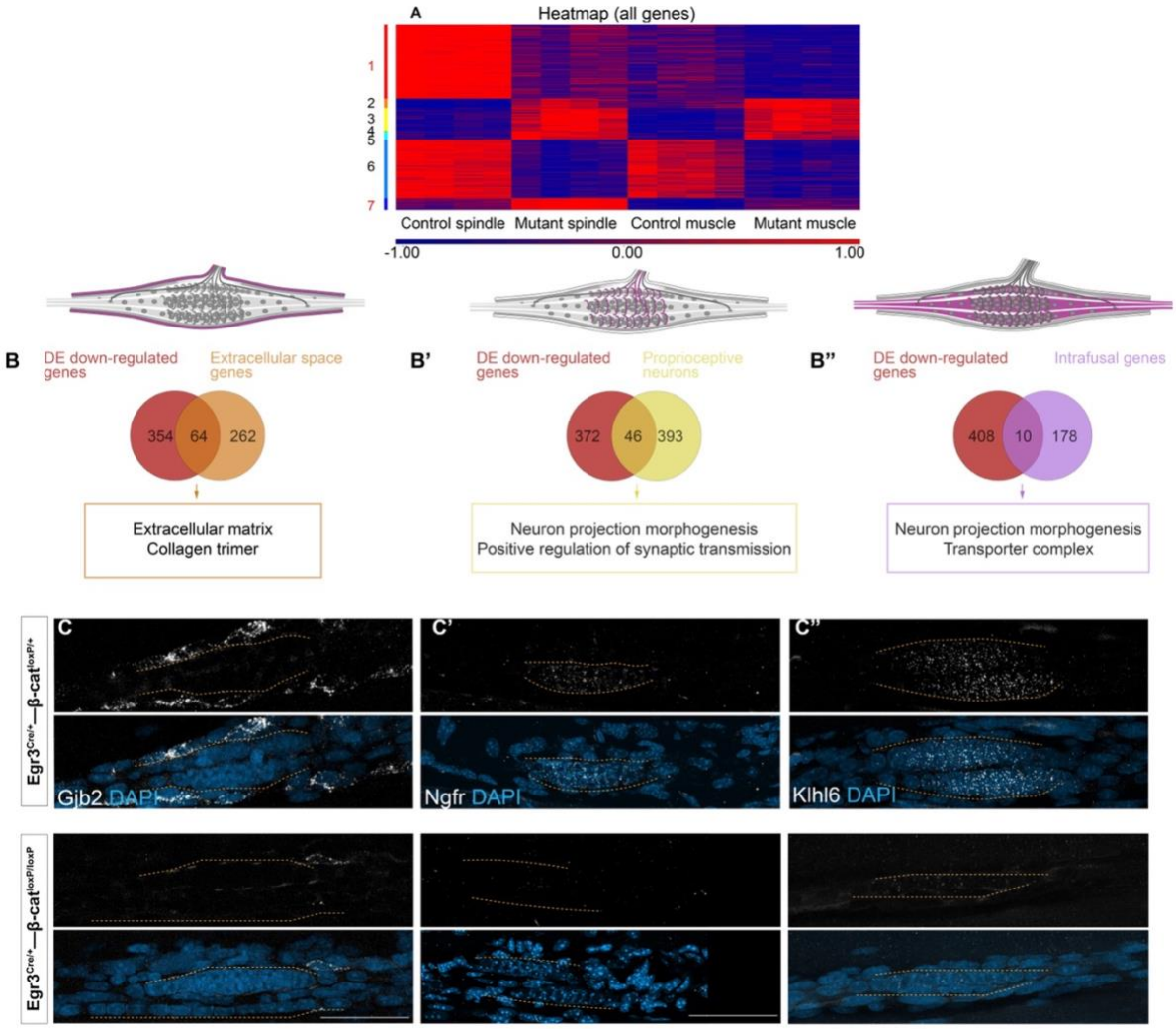

Figure 5. Transcriptomic analysis of *Egr3-β-catenin* mutant and control tissues. (A) Heatmap of DE between control and mutant spindle and muscle tissues. (B-B'') Top: schematic representation of the tissue being analyzed in purple. Middle: A Venn diagram showing overlapping genes between DE downregulated genes in mutant spindles and extracellular space genes (B), proprioceptive neurons (B') and intrafusal genes (B''). Bottom: Gene ontology (GO) analysis for enriched biological processes in each the overlapping datasets. (C-C'') Confocal images of whole-mount EDL muscle processed with HCR against Gjb2 in the capsule cells (C), Ngfr in the proprioceptive nerve (C') and Klhl6 in the intrafusal fibers (C'').

The molecular changes underlying the role of β-catenin in muscle spindle development.

303 To identify molecular signatures underlying the phenotypes in β-catenin mutated muscle spindles,
304 we subjected the spindle-specific genes from cluster 1 to IPA. We find that the most affected
305 cellular pathways are connective tissue-related and neuronal (Table S5 and Figure 6A).
306 Connective tissue pathways contain terms such as "assembly of collagen fibrils and other
307 multimeric structures"; genes downregulated in mutant spindle include various collagens, fibulin,
308 and integrins, including *Col12a1* and *Col18a1*, and ECM genes, such as *Itgb4* and *Loxl4* (Figure
309 6B, Table S5). The neuronal pathways include terms like "axon guidance" and "synaptogenesis".
310 Genes that were downregulated in β-catenin mutant spindle include *Dlg4*, *Grin2d,* and *Stx1b*,
311 which are involved in synaptogenesis, as well as axon guidance-associated *Ntrk3* and *Ngfr* (Figure
312 6C, Table S5). Interestingly, our analysis also identified downregulation of genes encoding coupled
313 guidance ligands and receptors crucial to both synaptogenesis and axon guidance, including the
314 Eph-ephrin, neurexin-neuroligin, and semaphorin-plexin signaling pathways (Figure 6C'). These
315 findings are consistent with the phenotypes in β-catenin mutant spindles, including capsule and
316 sensory nerve defects.
317
318 In contrast to the sensory neurons and capsule cells, IPA analysis does not reveal a clear molecular
319 explanation for the intrafusal phenotype. The loss of nuclear aggregation in the equatorial region
320 of β-catenin mutant bag2 fibers led us to hypothesize that the affected genes might be specifically
321 expressed by nuclei within the equatorial region. To test this possibility, we cross-referenced the
322 list of 10 differentially expressed intrafusal fiber genes with a published dataset on the equatorial
323 region[22]. This analysis revealed three genes—*Igfn1*, *Lrtm1*, and *Klhl6*, that we described above.
324 Interestingly, *IGFN1* is an adhesion protein involved in myoblast fusion and differentiation[34],
325 while *LRTM1* is a transmembrane protein found at synapses[35]. Although we see changes in the
326 expression of several intrafusal fiber genes, which further expand our understanding of the
327 molecular phenotype of β-catenin mutant spindles, these changes do not explain the loss of nuclear
328 aggregation in the mutant spindles. Therefore, we investigated the expression of genes previously
329 shown to be important for nuclear arrangements during development, regeneration, and at
330 neuromuscular junctions (NMJ)[36]. Of the 29 relevant genes (Table S6), *Pard6g* and *Lmnb2* are
331 significantly downregulated in mutant spindles.
332 Overall, we establish Wnt/β-catenin as a key molecular component in the coordinated development
333 of the different muscle spindle tissues. Our transcriptional analysis of spindles from control and β-

catenin mutant mice sheds light on molecular mechanisms underlying spindle tissue development regulated by β-catenin, and reveals many genes and pathways not previously implicated in muscle spindle development.

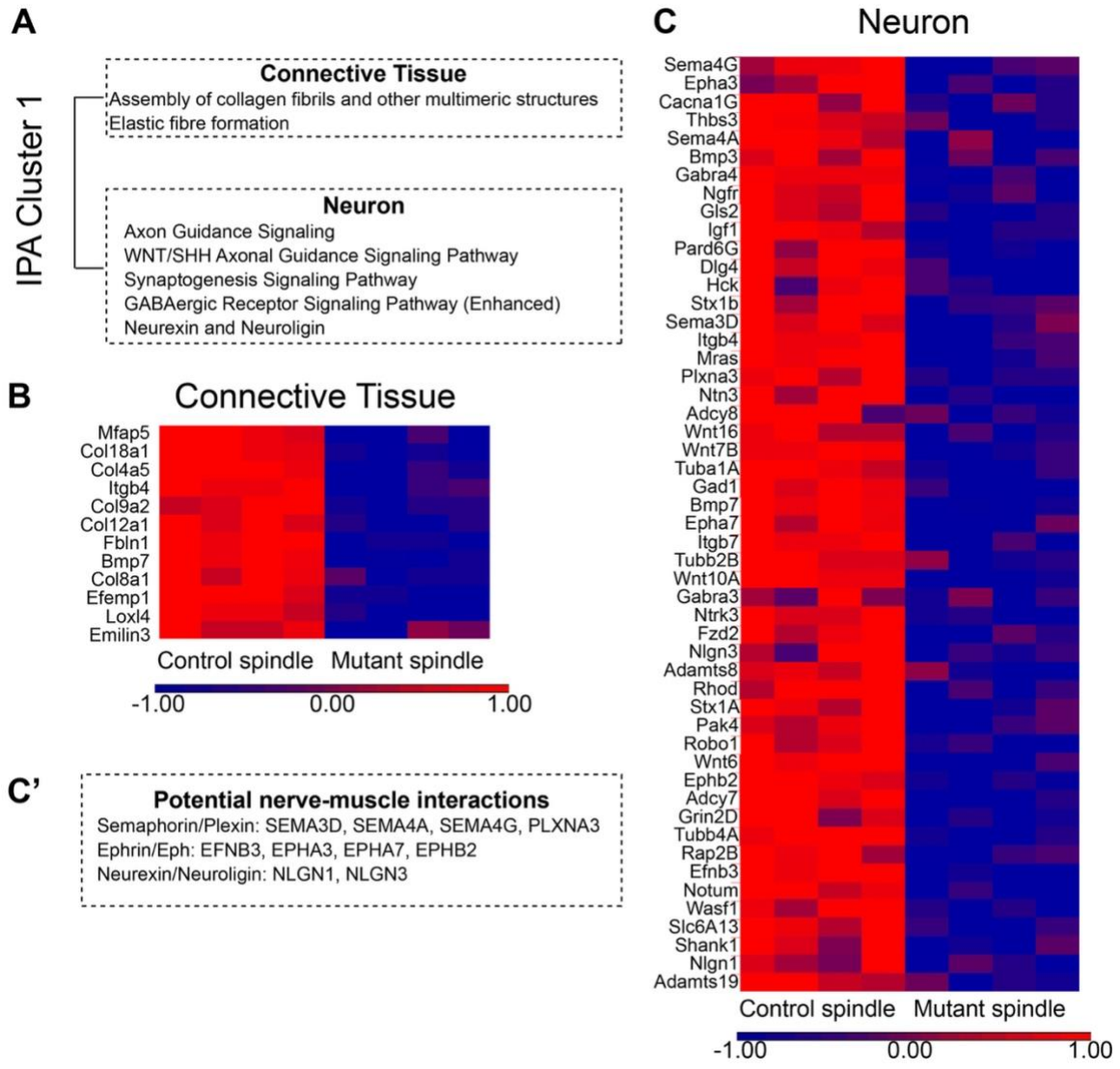

Figure 6. IPA analysis of muscle spindle-specific DE downregulated genes between *Egr3-β-catenin* mutants and controls. (A) IPA pathway analysis of genes from cluster 1 (Figure 5A). (B) DEG from connective tissue IPA pathways. (C) DEG from neuronal IPA pathways. (C') DEG from neuronal IPA pathways that show ligand-receptor interactions.

346 **Discussion**

347 Muscle spindles are the sensory receptors at the heart of proprioception, and yet surprisingly
348 little is known about the molecular basis of their development. Here, we show that Wnt/β-catenin
349 signaling is active in developing spindles and is required for proper development of specific
350 components of the spindle apparatus. Deletion of β-catenin from the embryonic capsule and
351 intrafusal fibers leads to malformations in the capsule, intrafusal fibers, and proprioceptive nerve
352 endings, suggesting both autonomous and non-autonomous regulatory roles in spindle
353 development. Specific deletion of β-catenin in postnatal muscle fibers disrupts the structure of
354 proprioceptive nerves, further supporting a non-autonomous role for intrafusal β-catenin in nerve
355 ending development. Finally, we use transcriptomic analysis of β-catenin mutant spindles to
356 reveal genetic mechanisms under β-catenin control that may guide muscle spindle development.

357

358 Outside of the initial steps during embryogenesis[7-9,11-16], muscle spindle development is poorly
359 studied, such that molecular mechanisms that coordinate the development of different spindle
360 tissue types are unknown. In that context, our finding that β-catenin is active throughout spindle
361 development in bag2 intrafusal fibers is interesting. Bag2 fibers are the first intrafusal fibers to
362 form[9] and, therefore, it is tempting to speculate that β-catenin activity in these fibers is part of the
363 coordinating mechanism.

364

365 Concurrently with the progression of intrafusal fiber development, proprioceptive neurons undergo
366 maturation to form the complex structure of the annulospiral endings[10]. Recently, we showed that
367 capsule development involves progressive waves of cell differentiation, moving from the center
368 of the spindle to its sides[11]. Our new finding that blocking β-catenin in intrafusal fibers and capsule
369 cells affects the development of all three spindle tissues supports its autonomous and non-
370 autonomous regulatory roles in spindle development.

371

372 Substantial evidence suggests that the muscle spindle capsule functions as a diffusion barrier,
373 similar to the blood-nerve barrier in peripheral nerves[37-39]. This requires a molecular mechanism
374 to ensure sufficient nutrient transport into the spindle. Our finding that the expression of *Gjb2*,
375 *Glut1* and *Stra6* is reduced in β-catenin mutants may provide insight into this mechanism. Studies
376 of inner ear development have shown that Gjb2 regulates glucose uptake, whereas Gjb2 and Glut1

377 were reported to cooperate in the rat cochlea to allow proper glucose transport[30]. Stra6 is a cell-
378 surface receptor that transfers retinol from retinol-binding protein into the cell, and is upregulated
379 by Wnt1 and Wnt3a[31]. Thus, these nutrient receptors and transporters are likely to be part of this
380 mechanism, regulated by β-catenin.
381
382 Capsule formation involves extensive ECM production. In β-catenin mutant spindles, we see that
383 many ECM building blocks are downregulated, including collagens, fibulin, and integrins, which
384 facilitate cell-ECM adhesion[40], and lysyl oxidase like 4 (loxl4), which catalyzes crosslinks in
385 collagens[41]. Together with the downregulation of versican, these results indicate deficits in ECM
386 synthesis and assembly, further supporting a role for β-catenin in capsule cell development.
387
388 While nuclear aggregation is a hallmark of intrafusal bag2 and bag1 fibers, little is known of the
389 molecular mechanism that regulates this process. Our finding that β-catenin activity is required for
390 nuclear aggregation exclusively during early stages of spindle development provides a molecular
391 entry point into this interesting process. Since nuclear movement, including aggregation, also
392 occurs during the formation of regular muscle fibers and in the NMJ[36], the underlying molecular
393 mechanism, which may involve β-catenin, could be shared. Our analysis of genes important for
394 nuclear movement reveals downregulation of *Pard6g* and *Lmnb2* in β-catenin mutant mice.
395 *Pard6g* encodes polarity proteins belonging to Par6 family, which interact with dynein/dynactin
396 at the nuclear envelope to drive nuclear centration during muscle development. *Lmnb2* encodes B
397 type nuclear lamin in the inner nuclear membrane, which is important for all nuclear movements,
398 including centration, spreading, dispersion and clustering, throughout muscle development,
399 maintenance and regeneration[36]. Moreover, we identified IGFN and KLHL6 as intrafusal genes.
400 IGFN1 is implicated in myoblast fusion and diffeentiation[34], suggesting its potential role in
401 intrafusal nuclear aggregation. The only function reported for KLHL6 is in B-cell survival and
402 maturation; however, other Kelch-like genes such as *Klhl19*, *Klhl40,* and *Klhl41* are important for
403 skeletal muscle development[33], suggesting a role for KLHL6 in intrafusal fiber development.
404 Further investigation into these genes may reveal the mechanism responsible for nuclear
405 aggregation in the muscle spindle.
406

407 At the interface with the intrafusal fibers, sensory endings undergo extensive morphological
408 changes during development to form the annulospiral loops[8,10]. The abnormal morphology of
409 annulospiral endings in β-catenin mutant spindles clearly suggests that β-catenin is necessary for
410 their maturation. However, we find that β-catenin is not active in sensory endings, implying a cell
411 non-autonomous regulatory mechanism. This possibility is supported by the abnormal morphology
412 of annulospiral endings upon blocking β-catenin expression only in intrafusal fibers.
413
414 The loss of β-catenin resulted in downregulation of several key signaling pathways that are
415 involved in axon guidance and synaptogenesis, including components of ephrin-Eph, semaphorin-
416 plexin and neurexin-neuroligin pathways. This may implicate these pathways in the regulation of
417 annulospiral loops, downstream of β-catenin. Interestingly, Ephrin-A/EphA signaling is involved
418 in proprioceptor muscle targeting[42]. Indeed, transcription of two of the downregulated guidance
419 genes, Eph receptor B2 and neuroligin-3, is regulated by the Wnt/β-catenin pathway in intestinal
420 stem cells and in hippocampal cells, respectively[43-44]. The three pathways share similar
421 mechanisms, involving receptors on one cell and ligands on the other[45-47]. The interaction of
422 receptors and ligands leads to downstream events, including attraction or repulsion of contacting
423 cells and synaptic cleft bridging. Similarly, the expression of *Ngfr* in intrafusal fibers and of its
424 ligands in spindles raises the possibility that some of these ligands interact with Ngfr on intrafusal
425 fibers to control the modeling of annulospiral loops. Overall, our results provide several molecular
426 entry points to study the formation of this interesting sensory structure and its connection with
427 intrafusal fibers.
428
429 In summary, we establish Wnt/β-catenin as a key component in the mechanism regulating the
430 coordinated development of the different muscle spindle components. The significance of our
431 findings extends beyond addressing the regulatory role of β-catenin in spindle development. Since
432 the molecular milieu of the spindle remains largely unexplored, our perturbation of β-catenin
433 followed by comparative transcriptome analysis reveals a new molecular landscape, illuminating
434 not only the function of β-catenin but also numerous previously unknown genes essential for
435 spindle biology. Moreover, this collection of new molecules sheds light on previously
436 unappreciated aspects of the tissues and processes involved in the functionality of this organ,
437 offering fresh insights into muscle spindle development and function.

Methods

Mouse lines

The generation of *Axin2-mGFP* (The Jackson Laboratory, #037313)[23], *calbindin-Cre*[22], *Egr3-Cre*[25], *HSA-MCM* (also known as Tg(ACTA1-cre/Esr1*)2Kesr/J; The Jackson Laboratory, #025750)[27], *Gli1-CreER*^{T2} (The Jackson Laboratory, #007913)[11], *Rosa26-tdTomato* (The Jackson Laboratory, #007909)[48] and *β-catenin*^{flox} (aka B6.129-*Ctnnb1*^{tm2Kem}/KnwJ; The Jackson Laboratory, #004152)[26] has been described previously. For HCR of *Wnts*, *calbindin-Cre* mice and *Gli1-CreER*^{T2} mice were crossed with *Rosa26-tdTomato* mice. To induce Cre-mediated recombination in *Gli1-CreER*^{T2}*:Rosa26-tdTomato* mice, 200 mg/kg of 50 mg/mL tamoxifen (Sigma-Aldrich, T5648) dissolved in corn oil (Sigma-Aldrich, C-8267) was administered at indicated age via oral gavage (Fine Science Tools). To generate *Egr3* control and mutant mice, *Egr3-Cre* mice were crossed with *β-catenin*$^{flox/flox}$*, Rosa26-tdTomato* mice. To generate HSA control and mutant mice, *HSA-MCM* mice were crossed with *β-catenin*$^{flox/flox}$*, Rosa26-tdTomato* mice. To induce Cre-mediated recombination, 7 µL of 50 mg/mL tamoxifen in corn oil was administered by oral gavage for 3 consecutive days starting from P5. All animals were sacrificed by CO_2 inhalation, fixed overnight shaking in 4% paraformaldehyde (PFA)/PBS at 4°C, washed in PBS and stored at 4°C in PBS. Mice were given free access to water and standard mouse chow with 12-h light/dark cycles. All animal procedures were approved by the Institutional Animal Care and Use Committee of Weizmann Institute. Ear genomic DNA was used for genotyping by PCR.

Immunofluorescence

For cryosection immunofluorescence, tissues were processed as previously described[11]. In brief, fixed deep masseter muscles were dissected and placed in 30% sucrose overnight with shaking. The muscles were then embedded in OCT and sectioned at 30 µm thickness using a cryostat. Cryosections were dried, post-fixed in 4% PFA, permeabilized with PBS containing 0.3% Triton X-100, washed with PBS containing 0.1% Tween-20 (PBST) and blocked with 7% goat/horse serum and 1% bovine serum albumin (BSA) in PBST. The sections were then incubated with primary antibodies (Table S7) overnight at 4°C, followed by a 1-hour incubation with secondary antibodies conjugated with fluorophores (Table S7) at room temperature. The sections were counterstained with DAPI and mounted with Immu-mount aqueous-based mounting medium

(Thermo Fisher Scientific). Imaging was performed with LSM 800 or LSM900 confocal microscope (Zeiss).

For whole-mount immunofluorescence, muscles were subjected to an optical tissue clearing protocol as described previously[11]. Shortly, fixed EDL muscles were dissected and embedded into an A4P0 hydrogel (4% acrylamide, 0.25% 2'-azobis[2-(2-imidazolin-2-yl)propane]dihydrochloride in PBS) with shaking at 4°C overnight. Then, samples were polymerized in hydrogel for 3 h at 37°C and the hydrogel was removed by washing in PBS. Next, samples were transferred to 10% SDS (pH 8.0) with 0.01% sodium azide, shaking gently at 37°C for 2 days. Cleared samples were then washed in wash buffer, blocked with CAS block for 5 h at 37°C with shaking, and incubated with primary antibodies (Table 1) for 4 days at 37°C with shaking. They were then incubated with secondary antibodies (Table 1) and DAPI (8 µg/ml) for 2 days at 37°C with shaking. For clearing and mounting, samples were incubated in 500 µl of refractive index matching solution (RIMS; 74% wt/vol Histodenz in 0.02 M phosphate buffer) for 1 day at room temperature with gentle shaking. Samples were then embedded in RIMS and imaged using a Zeiss LSM800 or LSM900 confocal microscope. Images were processed with ImageJ 1.51 (National Institute of Health).

Single-molecule *in situ* hybridization chain reaction (HCR)

For cryosection HCR, deep masseter muscles were dissected, transferred to 30% sucrose overnight with shaking, then embedded in OCT and sectioned at a thickness of 30 µm using cryostat. Cryosections were processed for HCR smFISH as described in http://www.molecularinstruments.com. Briefly, slides were incubated with the specified probes overnight, washed and incubated with fluorophore-conjugated amplifiers. The sections were counterstained with DAPI, mounted with Immuno-mount, and imaged using a LSM 800 or LSM900 confocal microscope (Zeiss).

For whole-mount HCR, EDL muscles were dissected, subjected to optical tissue clearing, and processed for HCR smFISH as previously described[49]. Shortly, samples were incubated in probe solution overnight at 37 °C, washed, and then incubated with fluorescent amplifiers overnight at room temperature. Next, samples were washed and counterstained with DAPI (8 µg/ml) for 2 h at room temperature. Finally, samples were moved to 500 µl RIMS overnight at room temperature

and embedded in RIMS for imaging. Images were captured by LSM800 or LSM900 confocal microscope (Zeiss).

Bulk RNA sequencing

For RNA-seq analysis, tissues were processed as described before[11]. Deep masseter muscles, each containing about 20 spindles, were dissected from *Egr3-Cre;TdTom;catenin* control and mutant mice. Then, bundles of spindles and adjacent extrafusal muscle fibers were micro-dissected and frozen on dry ice. For each sample, we pooled the same tissue from two animals of the same genotype. Each genotype had four replicates for each tissue, four samples of spindles and four samples of extrafusal fibers for both mutants and controls.

Muscle spindle isolation

To isolate muscle spindles from deep masseter muscles, spindles were dissected in ice-cold Liley's solution (Liley, 1956) ($NaHCO_3$ 1 g, KCl 0.3 g, KH_2PO_4 0.13 g, NaCl 0.2 g, $CaCl_2$ 1 M 2 ml in total of 1 L DDW).

Sample preparation

Total RNA was extracted using TRIzol Reagent followed by chloroform phase separation and processing with the RNeasy Micro kit (Qiagen). The quality and concentration of RNA were assessed using NanoDrop and TapeStation. RNA-seq libraries were generated at the Crown Genomics Institute of the Nancy and Stephen Grand Israel National Center for Personalized Medicine, Weizmann Institute of Science, following the INCPM-mRNA-seq protocol. The libraries were quantified by Qubit and TapeStation. Sequencing was conducted on an Illumina NextSeq instrument with a single end 75 cycles high output kit, yielding approximately ~20 M reads or more per sample.

Analysis of RNA-seq data

Transcriptomic data from four replicates of spindle samples and four muscle samples from mutants and controls were analyzed. A user-friendly Transcriptome Analysis Pipeline (UTAP) version 1.10.1 was used for analysis[50]. Reads were mapped to the *M. musculus* genome (GRCm38), using STAR (v2.5.2b)[51] and RefSeq annotation. Only reads with unique mapping were considered for further analysis. Gene expression was calculated and normalized using DESeq2 version 1.16.1[52], using only genes with a minimum of five reads in at least one sample. Raw p-values were adjusted for multiple testing[53]. A gene was considered differentially expressed if it passed the following

thresholds: minimum mean normalized expression of 5, adjusted p-value ≤0.05, and absolute value of log2 fold change ≥1. Ingenuity pathway analysis[21] and Partek[29] were used for analysis.

Statistical analyses

All measurements were taken with confocal Z-stack projections through ImageJ 1.51. At least eight spindles from three animals of each genotype were measured. Differences were assessed by comparing animals with different genotypes with a linear mixed-effects model (with animal as a random factor) and statistical significance was defined as a p-value lower than 0.05. The analyses were done in R, v. 4.4.2, using the packages 'lmerTest' and 'lme4'.

Reference

1. Proske, U., & Gandevia, S. C. (2012). The proprioceptive senses: their roles in signaling body shape, body position and movement, and muscle force. *Physiological Reviews*, *92*(4), 1651–1697. https://doi.org/10.1152/PHYSREV.00048.2011
2. Dietz, V. (2002). Proprioception and locomotor disorders. *Nature Reviews Neuroscience 2002 3:10*, *3*(10), 781–790. https://doi.org/10.1038/nrn939
3. Bornstein, B., Konstantin, N., Alessandro, C., Tresch, M. C., & Zelzer, E. (2021). More than movement: the proprioceptive system as a new regulator of musculoskeletal biology. *Current Opinion in Physiology*, *20*, 77–89. https://doi.org/10.1016/J.COPHYS.2021.01.004
4. Assaraf, E., Blecher, R., Heinemann-Yerushalmi, L., Krief, S., Carmel Vinestock, R., Biton, I. E., Brumfeld, V., Rotkopf, R., Avisar, E., Agar, G., & Zelzer, E. (2020). Piezo2 expressed in proprioceptive neurons is essential for skeletal integrity. *Nature Communications 2020 11:1*, *11*(1), 1–15. https://doi.org/10.1038/s41467-020-16971-6
5. Blecher, R., Krief, S., Galili, T., Assaraf, E., Stern, T., Anekstein, Y., Agar, G., & Zelzer, E. (2017). The Proprioceptive System Regulates Morphologic Restoration of Fractured Bones. *Cell Reports*, *20*(8), 1775. https://doi.org/10.1016/J.CELREP.2017.07.073
6. Blecher, R., Krief, S., Galili, T., Biton, I. E., Stern, T., Assaraf, E., Levanon, D., Appel, E., Anekstein, Y., Agar, G., Groner, Y., & Zelzer, E. (2017). The Proprioceptive System Masterminds Spinal Alignment: Insight into the Mechanism of Scoliosis. *Developmental Cell*, *42*(4), 388-399.e3. https://doi.org/10.1016/J.DEVCEL.2017.07.022
7. Bewick, G. S., & Banks, R. W. (2015). Mechanotransduction in the muscle spindle. *Pflugers Archiv : European Journal of Physiology*, *467*(1), 175–190. https://doi.org/10.1007/S00424-014-1536-9
8. Kröger, S., & Watkins, B. (2021). Muscle spindle function in healthy and diseased muscle. *Skeletal Muscle 2021 11:1*, *11*(1), 1–13. https://doi.org/10.1186/S13395-020-00258-X
9. Milburn, A. (1973). The early development of muscle spindles in the rat. *Journal of Cell Science*, *12*(1), 175–195. https://doi.org/10.1242/JCS.12.1.175
10. Maedu, N., Osawa, K., Masuda, T., Hakeda, T., & Kumegawa, M. (1985). Postnatal development of the anulospiral endings of Ia fibers in muscle spindles of mice. *Acta Anatomica*, *124*(1–2), 42–46. https://doi.org/10.1159/000146093
11. Bornstein, B., Heinemann-Yerushalmi, L., Krief, S., Adler, R., Dassa, B., Leshkowitz, D., Kim, M., Bewick, G., Banks, R. W., & Zelzer, E. (2023). Molecular characterization of the intact mouse muscle spindle using a multi-omics approach. *ELife*, *12*. https://doi.org/10.7554/ELIFE.81843
12. Chen, H. H., Hippenmeyer, S., Arber, S., & Frank, E. (2003). Development of the monosynaptic stretch reflex circuit. *Current Opinion in Neurobiology*, *13*(1), 96–102. https://doi.org/10.1016/S0959-4388(03)00006-0
13. Cheret, C., Willem, M., Fricker, F. R., Wende, H., Wulf-Goldenberg, A., Tahirovic, S., Nave, K. A., Saftig, P., Haass, C., Garratt, A. N., Bennett, D. L., & Birchmeier, C. (2013). Bace1 and Neuregulin-1 cooperate to control formation and maintenance of muscle spindles. *The EMBO Journal*, *32*(14), 2015. https://doi.org/10.1038/EMBOJ.2013.146

14. Leu, M., Bellmunt, E., Schwander, M., Fariñas, I., Brenner, H. R., & Müller, U. (2003). Erbb2 regulates neuromuscular synapse formation and is essential for muscle spindle development. *Development*, *130*(11), 2291–2301. https://doi.org/10.1242/DEV.00447
15. Hippenmeyer, S., Shneider, N. A., Birchmeier, C., Burden, S. J., Jessell, T. M., & Arber, S. (2002). A role for Neuregulin1 signaling in muscle spindle differentiation. *Neuron*, *36*(6), 1035–1049. https://doi.org/10.1016/S0896-6273(02)01101-7
16. Chen, H. H., & Frank, E. (1999). Development and specification of muscle sensory neurons. *Current Opinion in Neurobiology*, *9*(4), 405–409. https://doi.org/10.1016/S0959-4388(99)80061-0
17. Cao, R., Chen, P., Wang, H., Jing, H., Zhang, H., Xing, G., Luo, B., Pan, J., Yu, Z., Xiong, W.-C., & Mei, L. (2023). Intrafusal-fiber LRP4 for muscle spindle formation and maintenance in adult and aged animals. *Nature Communications 2023 14:1*, *14*(1), 1–17. https://doi.org/10.1038/s41467-023-36454-8
18. Clevers, H. (2006). Wnt/beta-catenin signaling in development and disease. *Cell*, *127*(3), 469–480. https://doi.org/10.1016/J.CELL.2006.10.018
19. MacDonald, B. T., Tamai, K., & He, X. (2009). Wnt/beta-catenin signaling: components, mechanisms, and diseases. *Developmental Cell*, *17*(1), 9–26. https://doi.org/10.1016/J.DEVCEL.2009.06.016
20. Ashrafi, S., Lalancette-Hébert, M., Friese, A., Sigrist, M., Arber, S., Shneider, N. A., & Kaltschmidt, J. A. (2012). *Wnt7A Identifies Embryonic-Motor Neurons and Reveals Early Postnatal Dependence of-Motor Neurons on a Muscle Spindle-Derived Signal*. https://doi.org/10.1523/JNEUROSCI.1160-12.2012
21. QIAGEN Ingenuity Pathway Analysis algorithm (https://digitalinsights.qiagen.com/; Qiagen, Redwood City, CA; USA; Krämer et al., 2014).
22. Kim, M., Franke, V., Brandt, B., Lowenstein, E. D., Schöwel, V., Spuler, S., Akalin, A., & Birchmeier, C. (2020). Single-nucleus transcriptomics reveals functional compartmentalization in syncytial skeletal muscle cells. *Nature Communications 2020 11:1*, *11*(1), 1–14. https://doi.org/10.1038/s41467-020-20064-9
23. Wang, J., Song, W., Yang, R., Li, C., Wu, T., Dong, X. B., Zhou, B., Guo, X., Chen, J., Liu, Z., Yu, Q. C., Li, W., Fu, J., & Zeng, Y. A. (2021). Endothelial Wnts control mammary epithelial patterning via fibroblast signaling. *Cell Reports*, *34*(13), 108897. https://doi.org/10.1016/j.celrep.2021.108897
24. Walro, J. M., & Wang, J. (1995). Origin of Spindles in Developing Rat Hindlimb Muscles. *Alpha and Gamma Motor Systems*, 189–195. https://doi.org/10.1007/978-1-4615-1935-5_40
25. Fernandes, M. O., & Tourtellotte, W. G. (2015). Egr3-Dependent Muscle Spindle Stretch Receptor Intrafusal Muscle Fiber Differentiation and Fusimotor Innervation Homeostasis. *The Journal of Neuroscience*, *35*(14), 5566. https://doi.org/10.1523/JNEUROSCI.0241-15.2015
26. Brault, V., Moore, R., Kutsch, S., Ishibashi, M., Rowitch, D. H., McMahon, A. P., Sommer, L., Boussadia, O., & Kemler, R. (2001). Inactivation of the β-catenin gene by Wnt1-Cre-mediated deletion results in dramatic brain malformation and failure of craniofacial development. *Development*, *128*(8), 1253–1264. https://doi.org/10.1242/DEV.128.8.1253

27. McCarthy, J. J., Srikuea, R., Kirby, T. J., Peterson, C. A., & Esser, K. A. (2012). Inducible Cre transgenic mouse strain for skeletal muscle-specific gene targeting. *Skeletal Muscle*, *2*(1), 1–7. https://doi.org/10.1186/2044-5040-2-8/FIGURES/4
28. Li, X. M., Dong, X. P., Luo, S. W., Zhang, B., Lee, D. H., Ting, A. K. L., Neiswender, H., Kim, C. H., Carpenter-Hyland, E., Gao, T. M., Xiong, W. C., & Mei, L. (2008). Retrograde regulation of motoneuron differentiation by muscle β-catenin. *Nature Neuroscience 2008 11:3*, *11*(3), 262–268. https://doi.org/10.1038/nn2053
29. Partek, an Illumina company (2024). Partek™ Genomics Suite™ (Version 7.0) [Computer software]. https://www.partek.com/partek-genomics-suite/
30. Matsunami, T., Suzuki, T., Hisa, Y., Takata, K., Takamatsu, T., & Oyamada, M. (2006). Gap Junctions Mediate Glucose Transport Between GLUT1-Positive and -Negative Cells in the Spiral Limbus of the Rat Cochlea. *Cell Communication & Adhesion*, *13*(1–2), 93–102. https://doi.org/10.1080/15419060600631805
31. Dhokia, V., & Macip, S. (2021). A master of all trades – linking retinoids to different signalling pathways through the multi-purpose receptor STRA6. *Cell Death Discovery 2021 7:1*, *7*(1), 1–8. https://doi.org/10.1038/s41420-021-00754-z
32. Bruno, F., Abondio, P., Montesanto, A., Luiselli, D., Bruni, A. C., & Maletta, R. (2023). The Nerve Growth Factor Receptor (NGFR/p75NTR): A Major Player in Alzheimer's Disease. *International Journal of Molecular Sciences 2023, Vol. 24, Page 3200*, *24*(4), 3200. https://doi.org/10.3390/IJMS24043200
33. Gupta, V. A., & Beggs, A. H. (2014). Kelch proteins: emerging roles in skeletal muscle development and diseases. *Skeletal Muscle 2014 4:1*, *4*(1), 1–12. https://doi.org/10.1186/2044-5040-4-11
34. Li, X., Baker, J., Cracknell, T., Haynes, A. R., & Blanco, G. (2017). IGFN1_v1 is required for myoblast fusion and differentiation. *PLOS ONE*, *12*(6), e0180217. https://doi.org/10.1371/JOURNAL.PONE.0180217
35. Rudenko, G. (2017). Dynamic Control of Synaptic Adhesion and Organizing Molecules in Synaptic Plasticity. *Neural Plasticity*, *2017*(1), 6526151. https://doi.org/10.1155/2017/6526151
36. Cadot, B., Gache, V., & Gomes, E. R. (2015). Moving and positioning the nucleus in skeletal muscle – one step at a time. *Nucleus*, *6*(5), 373–381. https://doi.org/10.1080/19491034.2015.1090073
37. Kennedy, W. R., & Yoon, K. S. (1979). Permeability of muscle spindle capillaries and capsule. *Muscle & Nerve*, *2*(2), 101–108. https://doi.org/10.1002/MUS.880020204
38. Dow, P. R., Shinn, S. L., & Ovalle, W. K. (1980). Ultrastructural study of a blood-muscle spindle barrier after systemic administration of horseradish peroxidase. *American Journal of Anatomy*, *157*(4), 375–388. https://doi.org/10.1002/AJA.1001570406
39. Ovalle, W. K., & Dow, P. R. (1985). Morphological aspects of the muscle spindle capsule and its functional significance. *The Muscle Spindle*, 23–28. https://doi.org/10.1007/978-1-349-07695-6_1
40. Karamanos, N. K., Theocharis, A. D., Piperigkou, Z., Manou, D., Passi, A., Skandalis, S. S., Vynios, D. H., Orian-Rousseau, V., Ricard-Blum, S., Schmelzer, C. E. H., Duca, L., Durbeej, M., Afratis, N. A., Troeberg, L., Franchi, M., Masola, V., & Onisto, M. (2021). A guide to the composition and functions of the extracellular matrix. *The FEBS Journal*, *288*(24), 6850–6912. https://doi.org/10.1111/FEBS.15776

41. Ma, H. Y., Li, Q., Wong, W. R., N'Diaye, E. N., Caplazi, P., Bender, H., Huang, Z., Arlantico, A., Jeet, S., Wong, A., Emson, C., Brightbill, H., Tam, L., Newman, R., Roose-Girma, M., Sandoval, W., & Ding, N. (2023). LOXL4, but not LOXL2, is the critical determinant of pathological collagen cross-linking and fibrosis in the lung. *Science Advances*, *9*(21). https://doi.org/10.1126/SCIADV.ADF0133/SUPPL_FILE/SCIADV.ADF0133_SM.PDF
42. Lai, K. O., Ip, F. C. F., Cheung, J., Fu, A. K. Y., & Ip, N. Y. (2001). Expression of Eph Receptors in Skeletal Muscle and Their Localization at the Neuromuscular Junction. *Molecular and Cellular Neuroscience*, *17*(6), 1034–1047. https://doi.org/10.1006/MCNE.2001.0997
43. Batlle, E., Henderson, J. T., Beghtel, H., Van den Born, M. M. W., Sancho, E., Huls, G., Meeldijk, J., Robertson, J., Van de Wetering, M., Pawson, T., & Clevers, H. (2002). β-Catenin and TCF Mediate Cell Positioning in the Intestinal Epithelium by Controlling the Expression of EphB/EphrinB. *Cell*, *111*(2), 251–263. https://doi.org/10.1016/S0092-8674(02)01015-2
44. Medina, M. A., Andrade, V. M., Caracci, M. O., Avila, M. E., Verdugo, D. A., Vargas, M. F., Ugarte, G. D., Reyes, A. E., Opazo, C., & De Ferrari, G. V. (2018). Wnt/β-catenin signaling stimulates the expression and synaptic clustering of the autism-associated Neuroligin 3 gene. *Translational Psychiatry 2018 8:1*, *8*(1), 1–12. https://doi.org/10.1038/s41398-018-0093-y
45. Egea, J., & Klein, R. (2007). Bidirectional Eph-ephrin signaling during axon guidance. *Trends in Cell Biology*, *17*(5), 230–238. https://doi.org/10.1016/j.tcb.2007.03.004
46. Craig, A. M., & Kang, Y. (2007). Neurexin–neuroligin signaling in synapse development. *Current Opinion in Neurobiology*, *17*(1), 43–52. https://doi.org/10.1016/J.CONB.2007.01.011
47. Koropouli, E., & Kolodkin, A. L. (2014). Semaphorins and the dynamic regulation of synapse assembly, refinement, and function. *Current Opinion in Neurobiology*, *27*, 1–7. https://doi.org/10.1016/J.CONB.2014.02.005
48. Madisen, L., Zwingman, T. A., Sunkin, S. M., Oh, S. W., Zariwala, H. A., Gu, H., Ng, L. L., Palmiter, R. D., Hawrylycz, M. J., Jones, A. R., Lein, E. S., & Zeng, H. (2009). A robust and high-throughput Cre reporting and characterization system for the whole mouse brain. *Nature Neuroscience 2009 13:1*, *13*(1), 133–140. https://doi.org/10.1038/nn.2467
49. Markman, S., Zada, M., David, E., Giladi, A., Amit, I., & Zelzer, E. (2023). A single-cell census of mouse limb development identifies complex spatiotemporal dynamics of skeleton formation. *Developmental Cell*, *58*(7), 565-581.e4. https://doi.org/10.1016/J.DEVCEL.2023.02.013
50. Kohen, R., Barlev, J., Hornung, G., Stelzer, G., Feldmesser, E., Kogan, K., Safran, M., & Leshkowitz, D. (2019). UTAP: User-friendly Transcriptome Analysis Pipeline. *BMC Bioinformatics*, *20*(1), 1–7. https://doi.org/10.1186/S12859-019-2728-2/TABLES/1
51. Dobin, A., Davis, C. A., Schlesinger, F., Drenkow, J., Zaleski, C., Jha, S., Batut, P., Chaisson, M., & Gingeras, T. R. (2013). STAR: ultrafast universal RNA-seq aligner. *Bioinformatics*, *29*(1), 15–21. https://doi.org/10.1093/BIOINFORMATICS/BTS635
52. Ahn, S., & Joyner, A. L. (2004). Dynamic Changes in the Response of Cells to Positive Hedgehog Signaling during Mouse Limb Patterning. *Cell*, *118*(4), 505–516. https://doi.org/10.1016/J.CELL.2004.07.023

53. Benjamini, Y., & Hochberg, Y. (1995). Controlling the False Discovery Rate: A Practical and Powerful Approach to Multiple Testing. *Journal of the Royal Statistical Society Series B: Statistical Methodology*, *57*(1), 289–300.

Declaration of interests

The authors declare no competing interests.